PROTEINS: Structure, Function, and Genetics 7:156–171 (1990)

β-Lactamase of *Bacillus licheniformis* 749/C at 2 Å Resolution

Paul C. Moews,[1] James R. Knox,[1] Otto Dideberg,[2] Paulette Charlier,[2] and Jean-Marie Frère[3]

[1]Department of Molecular and Cell Biology, The University of Connecticut, Storrs, Connecticut 06269, [2]Department of Crystallography, Institute of Physics, B5, and [3]Department of Enzymology, Institute of Chemistry, B6, Université de Liège, Sart Tilman, Liège, Belgium

ABSTRACT **Two crystal forms (A and B) of the 29,500 Da Class A β-lactamase (penicillinase) from *Bacillus licheniformis* 749/C have been examined crystallographically. The structure of B-form crystals has been solved to 2 Å resolution, the starting model for which was a 3.5 Å structure obtained from A-form crystals. The β-lactamase has an α + β structure with 11 helices and 5 β-strands seen also in a penicillin target DD-peptidase of *Streptomyces* R61.[1] Atomic parameters of the two molecules in the asymmetric unit were refined by simulated annealing at 2.0 Å resolution. The R factor is 0.208 for the 27,330 data greater than 3σ(*F*), with water molecules excluded from the model. The catalytic Ser-70 is at the N-terminus of a helix and is within hydrogen bonding distance of conserved Lys-73. Also interacting with the Lys-73 are Asn-132 and the conserved Glu-166, which is on a potentially flexible helix-containing loop. The structure suggests the binding of β-lactam substrates is facilitated by interactions with Lys-234, Thr-235, and Ala-237 in a conserved β-strand peptide, which is antiparallel to the β-lactam's acylamido linkage; an exposed cavity near Asn-170 exists for acylamido substituents. The reactive double bond of clavulanate-type inhibitors may interact with Arg-244 on the fourth β-strand. A very similar binding site architecture is seen in the DD-peptidase.[1]**

Key words: β-lactamase, penicillinase, penicillin-binding protein, penicillin antibiotics, X-ray diffraction, protein structure prediction

INTRODUCTION

The bacterial β-lactamase enzymes (EC 3.5.2.6) hydrolyze antibiotics of the β-lactam family (penicillins, cephalosporins, monobactams) to inactive products.

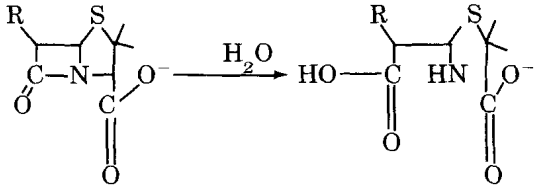

Their growing incidence in the clinical environment and the need to design enzyme-resistant penicillins have made necessary study of their structure and function at the molecular level.[2–6] Most β-lactamases characterized to date contain a reactive serine at the catalytic site. The serine enzymes are grouped into classes A, C, and now D, depending on their amino acid sequences and specificity for penicillins or cephalosporins. The sequences contain no invariant histidine, so that a mechanistic relationship with classical serine proteases is unclear. Crystallographic structure determinations at low to moderate resolutions have been published on representative β-lactamases from classes A and C,[1,7–11] and from a nonhomologous β-lactamase in class B which requires a catalytic zinc.[12]

Evidence for the ancestral derivation of β-lactamases from penicillin-inhibited cell wall synthesizing enzymes has been presented by Kelly et al.,[1] who discovered a tertiary structure resemblance between the two types of enzyme, represented by a class A β-lactamase from *Bacillus licheniformis* 749/C and a D-alanyl-D-alanine carboxypeptidase/transpeptidase from *Streptomyces* R61. In that report, the 3.5 Å crystal structure of the 29,500 Da β-lactamase was compared in terms of sequence homology and secondary structure with the larger DD-peptidase. Both enzymes, though differing in size by 8000 Da, contained a common five-stranded antiparallel β-sheet and a helical cluster arrangement which could be superimposed. Similar conclusions were drawn by Samraoui et al.[11] who pointed out the structural similarity between another class A β-lactamase from *Bacillus cereus* 569 and the DD-peptidase from *S.* R61. A later report,[13] based on quantitative sequence alignments, extended the ancestral linkages throughout the larger family of all penicillin-recognizing enzymes.

Received December 9, 1988; revision accepted October 27, 1989.

Address reprint requests to Dr. James R. Knox, Department of Molecular and Cell Biology, The University of Connecticut, 75 North Eagleville Rd.; Storrs, CT 06269.

Abbreviations used: PBP, penicillin-binding protein; PEG, polyethylene glycol; ISIR, image-enhaced single isomorphous replacement; SIR, single isomorphous replacement.

TABLE I. Crystal Parameters of *B. licheniformis* 749/C β-Lactamase

Crystal form	Cell dimensions (Å)				Space group	Volume (Å^3)	Molecules per asymmetric unit
	a	*b*	*c*	β(°)			
A	66.9	94.4	43.4	104.5	$P2_1$	264,900	2
B	66.8	90.7	43.6	104.5	$P2_1$	255,500	2

There are two crystal forms (A and B) of the exocellular β-lactamase from *B. licheniformis*. The structure of the A-form was solved at 3.5 Å resolution,[1] but crystals became harder to grow. Shortly afterward B-form crystals were obtained which were suitable for the collection of 2.0 Å data. It was expected that it would be possible to phase the B-form crystals using the A-form solution, and this has been achieved by a combination of image-enhanced single isomorphous replacement (ISIR)[14] and molecular replacement. A β-lactam substrate, benzylpenicillin, has been fitted to the binding site near the reactive Ser-70 using crystallographic information obtained from high-resolution maps of β-lactams complexed with the related DD-peptidase of *S.* R61.[15,16]

CRYSTALLIZATION METHODS

The magnoconstitutive strain 749/C of *B. licheniformis* was a gift of Dr. M. Sargent, National Institute of Medical Research, Mill Hill, U.K. The strain produces both membrane-bound and exocellular forms of a class A β-lactamase which has been sequenced.[17] After initial purification of the exocellular β-lactamase,[18] sequence analysis showed the presence of variable N-termini. After further purification with FPLC, about 90% of the material had an N-terminus KTE. Perhaps for this reason two forms of crystals resulted from crystallization in PEG media. The A-form of the enzyme was crystallized[19] from 15% (w/v) PEG 6000 in 50 mM sodium cacodylate at pH 5.5 by the vapor diffusion technique. Macroseeding was necessary to improve the size of the crystals. Later, another form, the B-form, was the predominant form which appeared under apparently identical growth conditions. Crystal parameters found for the two crystal forms are given in Table I. While it appears that the forms differ only by 4% in the b cell dimension, we find that the packing in the two crystal forms is quite different.

STRUCTURE DETERMINATION OF THE A-FORM

Because A-form crystals were obtained first, low-resolution data collection and heavy atom search were done with this form using a STOE-Siemens diffractometer and graphite monochromatized CuK_α radiation. Two equivalent reflections were measured using an omega step scan. An empirical absorption correction[20] was applied and 5,225 unique reflections resulted from 13,289 observations for the native data at 3.5 Å resolution. K_2PtCl_4 and $K_3UO_2F_5$ were found to form useful derivatives. Difference Patterson functions calculated with the K_2PtCl_4 (5 mM) data showed two principal sites. For $K_3UO_2F_5$ two principal sites were found for a 0.5 mM data set. Least-squares refinement gave the final heavy atom parameters in Table II.

Protein phase angles for the A-form were calculated by the method of Blow and Crick[21] and included the use of anomalous dispersion differences. The phases were refined using the image-enhanced multiple isomorphous replacement method.[14] After four cycles of refinement the figure of merit had increased from 0.62 to 0.76 and the overall residual had fallen from 0.41 to 0.29.

An electron density map was calculated which showed clearly the boundaries of the two molecules in the asymmetric unit. While the map was not of sufficient quality to position individual amino acids, it was possible to locate structural features using a ridge line representation of the electron density map[1] calculated with the program MKSKEL,[22] and interpreted on a graphics display terminal with the program GRINCH.[22]

STRUCTURE DETERMINATION OF THE B-FORM

Data from B-form crystals were collected at the Multiwire Area X-Ray Diffractometer Facility at the University of Virginia.[23] From a native crystal (0.10 × 0.30 × 0.50 mm) at pH 5.5, 53,000 intensities were measured at 21°C from 6.0 to 2.0 Å resolution with two overlapping multiwire detectors. A stepped phi scan was used with a step size of 0.05° and a count time of 25 seconds per step. All of the native B-form data were collected from one crystal in 3 days using nickel-filtered CuK_α X-radiation from a sealed-tube source. In the resolution range 6.0–3.0 Å, 97% of the observations were above background by three times their estimated error, and from 3.0 to 2.0 Å, 90% were significantly above background. Merging and symmetry averaging of multiple measurements from three chi settings of the native crystal produced 29,300 unique intensities and a discrepancy index $R = \Sigma|Ih_i - Ih_{aver}|/\Sigma Ih_i$

TABLE II. A-Form Heavy-Atom Parameters From Least-Squares Refinement

Derivative	$R(iso)$*	Site	Fractional coordinates			Fractional occupancy	R(LS)†
			x	y	z		
K_2PtCl_4	0.19	1	0.254	0.201	0.094	0.91	0.45
		2	0.178	0.000	0.196	0.72	
$K_3UO_2F_5$	0.21	1	0.700	0.095	0.929	0.43	0.59
		2	0.458	0.659	0.255	0.46	

*$R(iso)$ = $\Sigma\Delta|Fobs|/\Sigma|FP|$, where $\Delta|Fobs|$ = $|FPH| - |FP|$. $|FPH|$ and $|FP|$ are the measured structure amplitudes of the derivative and native protein in electrons.
†R(LS) = $\Sigma||FH| - |fH||/\Sigma|fH|$, where $|FH|$ is the lowest estimate of the heavy atom structure amplitude and $|fH|$ is the calculated structure amplitude for the heavy atom constellation.

= 0.057. Diffractometer data (6016 reflections) for a B-form native crystal were also collected to 3.0 Å. The merging residual when these data were scaled against the area detector data was 0.05. Low order reflections (900 at spacings > 5.0 Å) not collected on the area detector were used to complete the data set.

Area detector data were also collected from a K_2PtCl_4 derivative crystal of the B-form using graphite-monochromated CuK_α radiation on a rotating anode generator. In an omega step scan, a 0.05° step was counted for 20 seconds. From 39,194 observations throughout three phi settings of the crystal, 13,000 unique intensities in the range 6.0–2.5 Å resulted with a discrepancy index of 0.053.

Molecular Model

Atomic positions were not available for the low-resolution A-form structure. The solution, output by GRINCH, consists of nodes (electron density peaks) in a ridge line representation of the electron density map. Each node is assigned a value proportional to the electron density and only certain nodes are marked as being part of the molecule. These nodes (610) together with all nodes which were less than 4 Å away from a marked node (a total of 1669 nodes) were used as the model for the A-form structure and were considered atoms for structure factor calculations. Each node was assigned one of six scattering curves depending on the electron density associated with it.

A similar solution which traced the main structural features of the second molecule in the asymmetric unit of the A-form was also available. From the A-form solution, viewed on a three-dimensional display terminal, it was apparent that the two molecules were related by a noncrystallographic 2-fold axis which was nearly coincident with a^*; there was as well a translation of 3–4 Å along a^* required to superimpose the two molecules. The relationship was confirmed by the use of a program, written for the display terminal, which allows one to manually translate and rotate a molecule so as to superimpose it over a second molecule and then output the rotation matrix and translation vector required.

Rotation Function Results

Rotation functions were calculated using B. Craven's version (program ROTRAN) of Crowther's fast rotation function.[24] ROTRAN was run using the GRINCH model as the moving structure and either A-form data or B-form data as the fixed structure. Rotation functions calculated for the A-form had as the two strongest peaks (five to six times background) the expected solutions related by 180° rotation. Rotation functions calculated for the B-form were nearly identical. This unexpected result greatly simplified the determination of the relationship between the two crystal forms and the relationship between the four molecules in the unit cell. The relationship between an angle and an axis and the corresponding Eulerian angles was derived and is given in the Appendix. The rotational relationships given in the Appendix apply to both the A-form and B-form crystals; the values given in Table XI were used for the initial rotation parameters.

Before beginning translation searches the rotation solution was verified and refined using BRUTE.[25] Rotational searches were done using the A-form model and 1942 reflections from 12.5 to 5 Å resolution. The search was done over 64 orientations at 0.5° steps about the three orthogonal axes. The refined Eulerian angles for each of the two molecules in the asymmetric unit at the position of maximum correlation are given in Table III. The new rotational angles differ by an overall rotation of only 0.8° and 0.4°, respectively, from the original ones (see Appendix). The apparent large differences in Eulerian angles for molecule 1 is due to the equivalence of α and γ when β is near zero.

Translation Function Results

Translation searches were done with BRUTE.[25] Correlation coefficients and R-factors are calculated for each structure factor calculation over all possible translation solutions. After locating the two molecules on the xz plane, one molecule can be held and the other moved along the y axis to find the relative y positions of the two molecules. In the solutions given below an increment was added to y so that the

TABLE III. Refined Rotational Parameters for Molecules in the B-Form

Molecule	α	β	γ	Axis*	Angle	corr.†
1	341.3	0.79	18.4	−0.302 −0.898 0.312	0.8°	0.247
3	0.20	151.3	180.5	−0.569 −0.569 0.580	0.4°	0.208

*The axis and angle which takes the molecule after refinement to the molecule before refinement.
†Correlation coefficient.[25]

xz plane does not intersect the center of the molecules. The first translation searches were done on the A-form as the molecular positions were already known from our earlier work. Translation searches were then carried out on the B-form using data from 5.6 to 3.9 Å resolution (2,495 reflections). The translation function maps were nearly featureless except for peaks which corresponded to the solution. Once approximate answers were found using 1 Å steps, searches around the answer were carried out with 0.25 Å steps. The final values for the translations for the A- and B-forms are given in Table IV.

Figure 1 shows the packing, in space group $P2_1$, for the A-form and B-form, respectively. It is seen that the relative molecular positions are markedly different in the two crystal forms, even though their b cell dimensions differ by only 4%. Because the noncrystallographic diad is almost perpendicular to both the *b* and *c* axes, the symmetry of the A-form is pseudo 22_12, while that of the B-form is pseudo 2_12_12.

Molecular replacement phases for the B-form could now be calculated. Structure factor calculations were done using the X-ray System of programs.[26] For 3 Å data (9800 reflections) with $F > 0.21\,\bar{F}$ the initial residual was 0.51.

The B-form Heavy Atom Derivative

As molecular replacement phases at 3.5 Å resolution were now available for the B-form, a phased Fourier difference map was calculated to see if platinum positions were consistent with those indicated by the Patterson map. There were two principal peaks on the difference Fourier map which are related by the same rotation and translation that superimpose the two molecules in the asymmetric unit. A difference Patterson map contained two self vectors and as well the expected cross vectors consistent with the peaks on the molecular replacement Fourier map. The platinum positions were refined by a version of the program VICTOR[27] with the results in Table V. Phasing with this single derivative gave an overall figure of merit of 0.40 for 13,000 reflections at 2.5 Å resolution. Enhanced SIR phasing could now be done to extend the molecular replacement solutions.

REFINEMENT BY THE ISIR METHOD

A number of refinements using Wang's ISIR method[14] were carried out at resolutions of 4.7, 3.0, and 2.5 Å. Masks calculated directly by Wang's programs had intrusions of solvent regions into areas which were known to be protein from the molecular replacement results. Therefore the masks used to obtain maps for model fitting were calculated using the molecular replacement model.

In the masks the 610 nodes in the model, placed successively at each of the four molecular positions in the unit cell, were used to mark all grid points in an empty map within a certain distance of each node as belonging to protein. The distance from a node required to include a grid point in the mask was varied to include more or less of the points in the solvent region; the final value chosen marked 61% of the structure as belonging to protein, 39% to solvent. These values compare with 56 and 44% as estimated from the calculated partial specific volume of the protein. This mask was used to obtain B-form phases for 13,607 reflections at 2.5 Å resolution. After six cycles of refinement, phases had converged; the figure of merit increased from 0.48 to 0.73 and the residual fell from 0.54 to 0.24. A map based on phases output by the sixth cycle showed the trace of the main chain quite clearly, but some of the side chains in loops connecting secondary structural features were less apparent. The principal secondary structure elements, the 11 helices and 5-stranded β-sheet, were readily fitted into the map using the program FRODO.[28]

REFINEMENT BY SIMULATED ANNEALING

After a number of restrained least-squares structure factor refinement cycles using PROLSQ,[29] the structure was refined by simulated annealing using X-PLOR.[30,31] All data from 10.0 to 2.0 Å resolution were used (30,090 reflections). All reflections were equally weighted, and an overall isotropic temperature factor of 11 $Å^2$ was used initially. The model was improved by alternate cycles of manual rebuilding and simulated annealing refinement. After a number of trial calculations, the protocol described in Table VI was found to be effective; it requires about 3 hours of Cray Y-MP time. This protocol is similar to that used in the refinement of crambin,[31] except that the molecular dynamics steps have been replaced by the "slow cooling" step (3, Table VI) described in the X-PLOR manual.[32]

Read[33] has discussed the Fourier coefficients

TABLE IV. Translations for A- and B-Form Molecules

Molecule	*tx* (Å)	*ty* (Å)	*tz* (Å)	Correlation coefficient and sigma	Global mean correlation
1 (A-form)	19.0	22.0	19.0	0.29 (0.02)	0.17
3 (A-form)	14.0	74.0	11.0	0.23 (0.02)	0.15
1 (B-form)	28.75	20.0	7.25	0.25 (0.02)	0.15
3 (B-form)	3.75	70.75	22.25	0.21 (0.02)	0.13

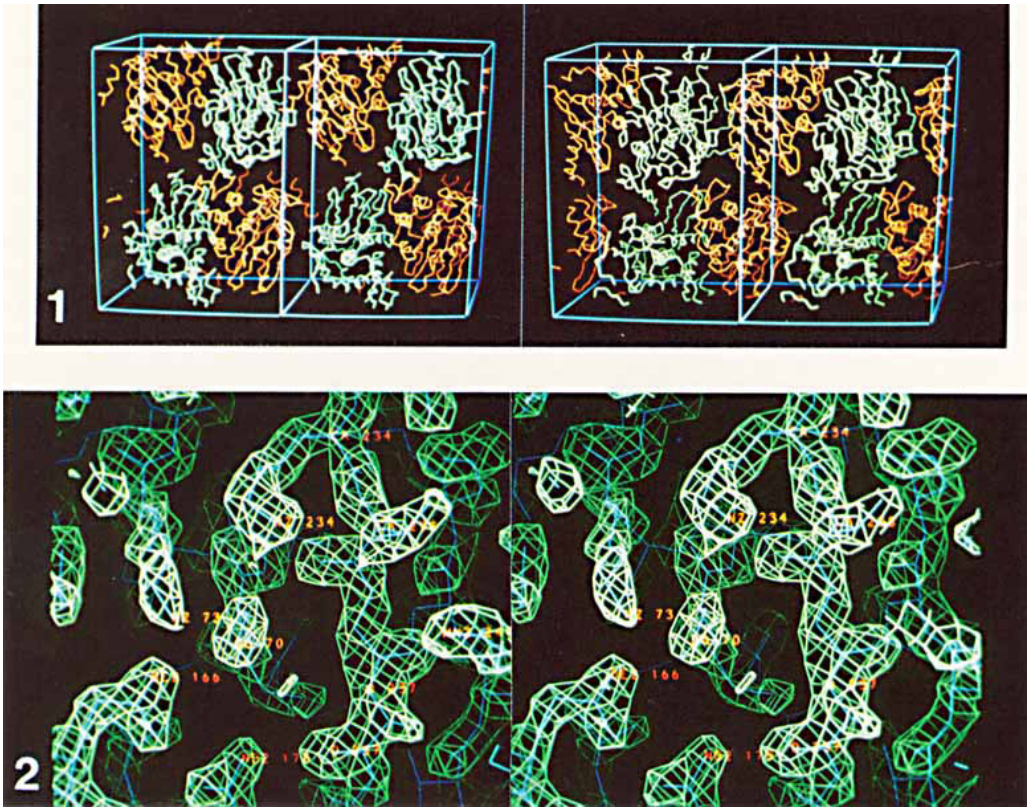

Fig. 1. Packing of β-lactamase molecules in A-form crystal (left) and B-form crystal (right). Space group equivalent α-carbons are drawn in same color. Both forms have space group $P2_1$. Cell dimensions differ by only 4% in length of *b* axis (vertical). View is down *c* axis.

Fig. 2. Electron density in active site region. The view direction is similar to that in Figs. 7 and 8, with β-strand b3 vertical. Fourier coefficients were calculated by Read's method[33] and are $2F_o - DF_c$.

TABLE V. B-Form Heavy Atom Parameters From Least-Squares Refinement

Derivative	*R*(*iso*)	Site	Fractional coordinates *x*	*y*	*z*	Occupancy electrons	B,Å^2	*R*(LS)*
K_2PtCl_4	0.15	1	0.9096	0.1042	0.3304	35.2	25.9	0.72
		2	0.4729	0.4089	0.0375	35.3	63.4	

*$R(LS) = \Sigma||FH| - |fH||/\Sigma|fH|$, where |FH| is the lowest estimate of the heavy atom structure amplitude and |fH| is the calculated structure amplitude for the heavy atom constellation.

which best remove model bias and has developed a program (SIGMAA) for calculating maps which minimize bias. Another method for removing model bias is the calculation of OMIT style maps as suggested by Bhat.[34] After each cycle of simulated annealing refinement, maps of both types were calculated using programs supplied by Read and Bhat. These methods work best if all data are included. In fact, the two types of maps, although calculated by quite different methods, were similar. However, model bias was apparent till the crystallographic *R* factor fell below 0.27. Possible modeling errors were

TABLE VI. Simulated Annealing Refinement Protocol

Stage	Description
1	Determination of W_A (ca. 300,000 kJ mol^{-1})
2	Minimization, 40 to 160 conjugate gradient steps, C^α restraints, tolerance = 0.05 Å, B = 11.0 $Å^2$
3	Molecular dynamics, "slow cooling," T = 4000–300° by 25° steps, tolerance = 0.2 Å, timestep = 0.0005 fsec, number of integration steps = 50
4	Minimization, 40 to 200 conjugate gradient steps, tolerance = 0.005 Å, B = 11.0 $Å^2$
5	Refinement of individual B factors

found from unlikely phi, psi, and omega angles, large temperature factors, and positions where the structures of the two molecules in the asymmetric unit differed. As the refinement progressed the RMS deviation between the main chain atoms (N,C^α,C) in the two independent molecules dropped from 0.72 to 0.25 Å. This behavior is similar to that observed by Baker[35] during the refinement of two independent molecules of azurin. Table VII summarizes the course of the refinement. The final R factor for all reflections in the range 10–2 Å is 0.219; if reflections with $F < 3\sigma(F)$ are omitted (2760 reflections) R is 0.208. The RMS deviation from standard geometry in the X-PLOR model is 0.022 Å for bond lengths and 3.5° for bond angles. This X-PLOR model and the residual were not significantly changed by four final cycles of PROLSQ refinement (RMS atom shift 0.07 Å), though RMS deviations from ideality of bonds, angles, and planes decreased to 0.014 Å, 3.0°, and 0.018 Å. Complete details of the deviation of the model from ideal geometry are given in Table VIII. Electron density at the penicillin binding site is pictured in Figure 2. Coordinates of α-carbon atoms have been deposited in the Brookhaven Protein Data Bank. Inclusion of water molecules and refinement of the hydrated structure is underway.

DISCUSSION OF THE STRUCTURE

Secondary Structure and Folding

The enzyme consists of an unusual arrangement of 11 helical segments and at least 5 antiparallel β-strands (Fig. 3) seen originally in the penicillin target DD-peptidase of *Streptomyces* R61[1,15,36,37] and more recently in several β-lactamases.[1,7,8,11] The 11 helices represent 45% of the structure. From the algorithms of Chou and Fasman[38] and Garnier et al.,[39] helical content had been predicted to be either 37 or 50%, respectively.[40] Somewhat less helix (28%) was predicted by Pain and Virden,[41] and as little as 22% was predicted by Bunster and Cid.[42] β-Strand is 25% of the polypeptide, though only 8 or 19% was predicted by the two algorithms. An alignment of observed and predicted secondary structure is shown in Figure 4. It is seen that the Chou and Fasman method tended to underpredict total amounts of α,β-structure, especially β-structure. The five longer β-strands form an antiparallel pleated sheet which is covered on the front face by the N- and C-terminal helices (a1 and a11). At the left edge and rear of the sheet are the remaining nine helices, with a single turn of helix at position 90. The reactive serine 70 is at the N-terminus of helix a2. A small imperfect portion of another β-sheet lies at the back of the enzyme; this sheet is comprised of three antiparallel segments 63–66, 159–163, and 178–183. The five N-terminal residues, KTEMK from 26 to 30 in the consensus numbering,[43,44] are not seen in the map for either molecule.

The crystallographic necessity to map two independent molecules in the asymmetric unit of the cell provided a useful check on our determination of chain folding and side chain conformation. The conformations of the two molecules are generally similar; the RMS difference in positions of α-carbon atoms in each of the two molecules is 0.26 Å. This similarity in folding shows that the two molecules in this crystal form are free of distorting packing forces, in agreement with the fact that the radius of gyration calculated from atomic coordinates of either molecule (17.8 Å) compares well with the measured value (17.3 ± 0.5 Å) from X-ray scattering in solution at pH 6.5.[45] Chain folding comparisons with two other Class A β-lactamases, from *Staphylococcus aureus* PC1 at 2.5A resolution[7] and *Streptomyces albus* G at 3.0 Å resolution[8] are shown in Figure 5. The RMS α-carbon difference is 1.3 Å for the *S. aureus* and *B. licheniformis* structures of higher resolution. Differences arise from the fact that the *S. aureus* enzyme contains several insertions and deletions after the a2-helix and has inserts at 239 and 252, while the *albus* G enzyme, unlike the other two enzymes, does not appear to have well-defined a3 and a7 helices. There is no obvious similarity in overall folding of these serine β-lactamases with the proteases of the papain, subtilisin,or chymotrypsin families. Rather, a striking similarity of the β-lactamases has been noted with the D-alanyl-D-alanine carboxypeptidase/transpeptidase of *S.* R61, as has the possible ancestral derivation of

TABLE VII. Course of X-PLOR Refinement

Cycle	Residual	RMS deviation from ideal bond length (Å)	RMS deviation from ideal bond angle (°)	RMS deviation between two molecules (Å) all atoms
1	0.296	0.031	5.5	1.27
3	0.275	0.026	4.8	1.25
5	0.249	0.026	4.4	0.86
7	0.225	0.023	3.6	0.67
8*	0.219	0.022	3.5	0.60

*Steps 2 and 3 of protocol omitted; minor corrections to model.

TABLE VIII. Deviations of Model From Ideal Geometry

	RMS deviation	Weighting parameters
Distances (Å)		
Bonds (1–2 neighbor)	0.014	0.014
Angles (1–3 neighbor)	0.046	0.027
Planar deviation	0.018	0.016
Chiral volume (Å^3)	0.21	0.13
Torsion angles (°)		
Planar	3.5	2.5
Staggered	22.8	30
Transverse	24.6	30
Contact (Å)		
Single torsion	0.17	0.35
Multiple torsion	0.20	0.35
H-bonds	0.18	0.35
Thermal factors (Å^2)		
Main chain (1–2 neighbor)	1.6	1.5
Main chain (1–3 neighbor)	2.3	2.0
Side chain bond	3.0	2.0
Side chain angle	4.4	3.0

the β-lactamases from the penicillin target enzymes.[1,8,11,13]

At least five Class A β-lactamases contain a covalent disulfide bond between residue 77 and 123. In this disulfide-free structure, the spatial location of these two residues on the inside of helices a2 and a4 nevertheless makes such a bond possible, as the α-carbons are separated by the 6.3 Å distance required for such a linkage.[46] By site-directed mutagenesis, Magdwick and Waley[47] introduced a single cysteine at one end of this site in the homologous *Bacillus cereus* 569/H β-lactamase I without loss of function.

Of the 29 amino acid positions which are invariant in the 12 known sequences of Class A β-lactamases,[43,44] seven are close to the antibiotic binding site; they are Ser-70, Lys-73, Ser-130, Glu-166, Leu-169, Lys-234, and Gly-236 (Fig. 3b). Many of the conserved residues are contained in or bordering the long strand from 66 to 91, which leads into and through the a2 helix. Around the conserved Leu-81 is a triad of three conserved leucines (91,199, and 207) which may anchor the C-terminal end of the important a2 helix. The two invariant prolines (107 and 252) are near turn positions of the chain.

Geometry of the Penicillin-Binding Site

Important segments of polypeptide which come together to form the penicillin-binding site are seen in Figure 6. Approach of β-lactam substrate to this site at the N-terminus of helix a2 is most likely from the bottom or lower front of the enzyme as pictured in Figure 3. Prior to and within the a2 helix is the conserved sequence Phe-66-x-x-x-ser-x-x-Lys-73, which is present in all Class A and C β-lactamase and some PBP sequences.[3] The Phe-66 is quite far (13 Å) from the reactive Ser-70, and lies against the back face of the β-sheet. The conserved Lys-73 in this sequence is actually adjacent to Ser-70 by virtue of being one turn up the a2 helix; the two residues are within hydrogen bonding distance. A schematic of potential interactions is seen in Figure 7.

Forming the right side of the binding site is the b3 strand, which contains the recurring sequence Asp-233, Lys(His)-234, Thr(Ser)-235, Gly-236. The latter three residues of this strand were first seen in the *S.* R61 DD-peptidase structure and exist in equivalent form in all penicillin-recognizing enzymes.[36] The ε-N of Lys-234 is at the upper right of the catalytic site far (4.8 Å) from the Ser-70 hydroxyl, and it is hydrogen bonded to conserved Ser-130. The next residue in the β-strand at position 235 is, in all sequences, a potential hydrogen binder, usually Ser or Thr. The conserved glycine at 236 is the residue closest to Ser-70; glycine is found in this position in all PBPs as well as in β-lactamases. Mutation at the variable position 237, at least in the homologous TEM plasmid β-lactamase, will alter substrate specificity.[13,48]

At the bottom of the binding site is the a7 helix and loop containing three invariant residues (Arg-164, Glu-166, and Leu-169). While Arg-164 projects into solvent, the conserved Glu-166 is associated with the active site via a weak interaction with Lys-73 at 3.2 Å, and a stronger one with Asn-170 at 2.9 Å. Also in this loop is the (almost invariant) glutamic acid 168, which, upon being derivatized by a carbodiimide, caused a 50% loss in activity of the homologous *B. cereus* 569/H/9 β-lactamase I.[49] However, because the carboxyl group of Glu-168 extends from the bottom of helix a7 into the solvent, such an effect on activity is difficult to understand.

Two short segments of polypeptide chain exist at the left of the binding site. One segment is the interhelix loop 126–133. The loop contains the conserved Ser-130 and Asp-131, the former being near three important residues: Ser-70, Lys-73, and Lys-234. The hydrogen bonding of Ser-130 and Lys-234 may aid the correct positioning of the substrate-binding b3 strand relative to the catalytic a2 helix (see below). The Asp-131, however, is directed away from the catalytic residues and may fulfill a subtle structural role. Asn-132 projects into the binding

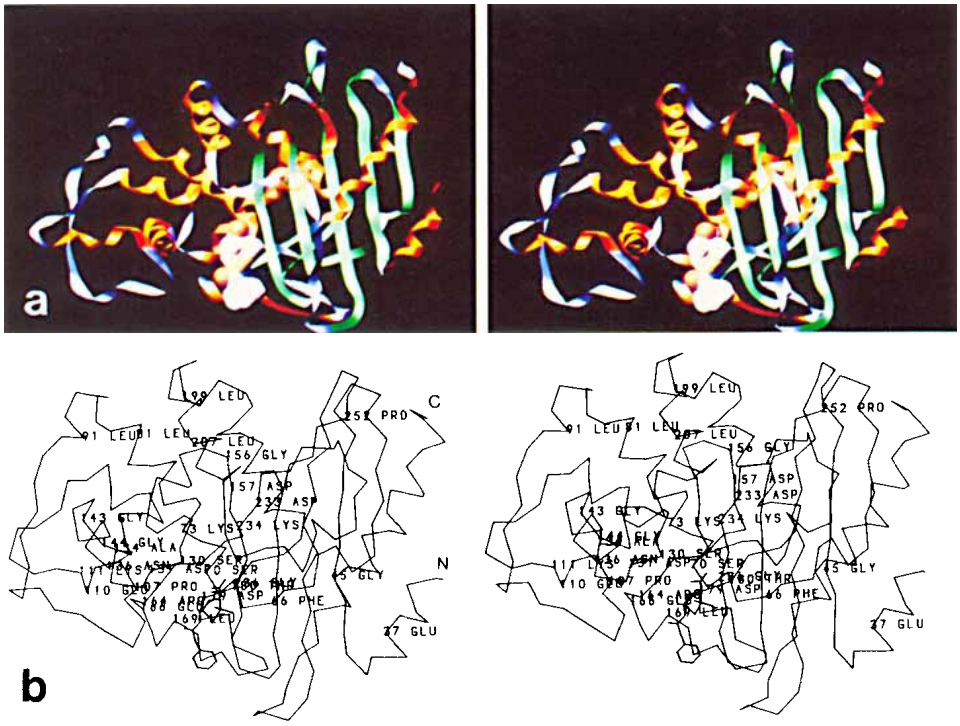

Fig. 3. **(a)** Ribbon representation of β-lactamase folding. Helical and β-strand segments are colored rust and green, respectively. Penicillin G is shown in binding site. (Figure is a VIEW diagram, courtesy of Mark Harris and David Chen, Department of Computer Sciences at the University of North Carolina.) **(b)** α-carbon backbone of *B. licheniformis* β-lactamase showing locations of the 29 invariant residues in Class A β-lactamases. Numbering is from Ambler[43] and Coulson[44] and runs from 31 to 295 in this plot. With this numbering, gaps occur at positions 58, 84–85, and 239. Five N-terminal residues from 26 are not seen in electron density map.

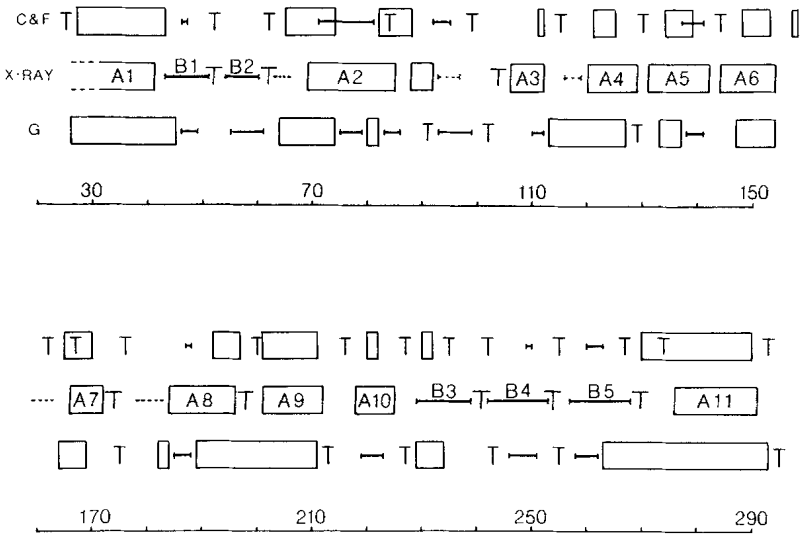

Fig. 4. Secondary structure of *B. licheniformis* β-lactamase (center) compared with structure predicted by methods of Chou and Fasman[38] (top) and Garnier et al.[39] (bottom). Boxes, bars, and T symbols represent helix, β-strand, and turn regions. Dashed bars in the X-ray line are short strand segments; blank regions are undefined structure. The reactive serine is at position 70. The five N-terminal residues are not seen in map.

site and may interact with β-lactam substrates. The second segment, the loop from 103 to 106 on the lower front face of the molecule places another functionality, Asn-104, near the bound substrate.

Penicillin Orientation in the Binding Site

High-resolution crystallographic maps exist for penicillin and cephalosporin complexes of the struc

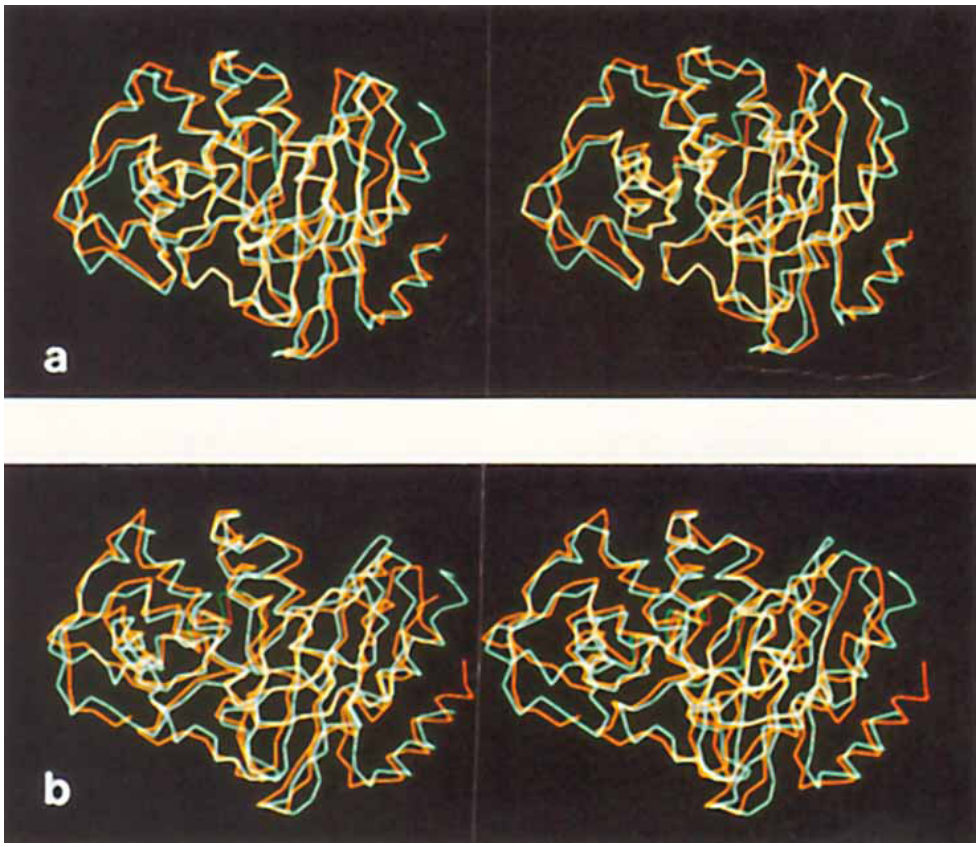

Fig. 5. α-Carbon backbone comparison of three Class A β-lactamases. **(a)** *B. licheniformis* (green) and *S. aureus* enzyme (red).[7] **(b)** *B. licheniformis* (green) and *S. albus* G enzyme (red).[8]

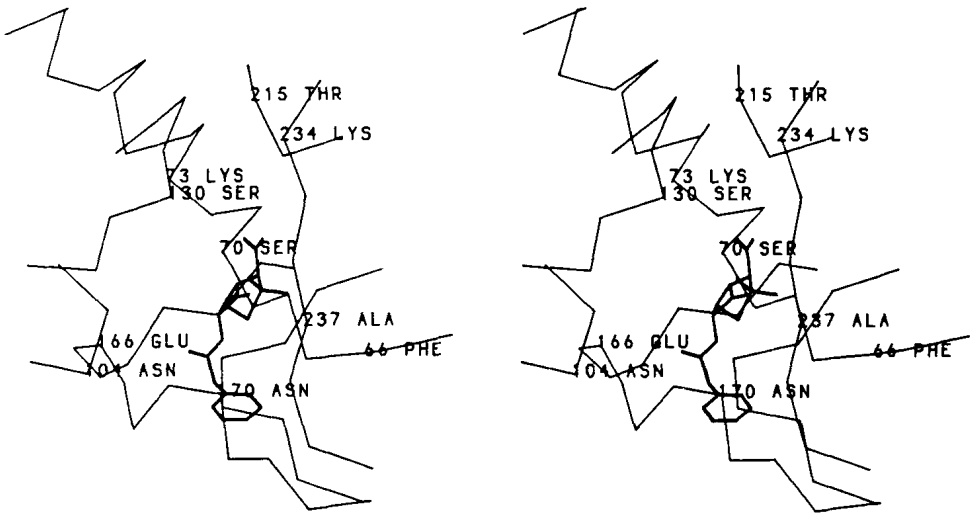

Fig. 6. Polypeptide segments near the β-lactam binding site: residues 64 to 83 in a2 helix, 103 to 106 before a3 helix, 126 to 133 between a4 and a5 helices, 159 to 182 in a7 helix/loop, 214 to 217 after a9 helix, and 233 to 241 in b3 strand. Penicillin G is also shown.

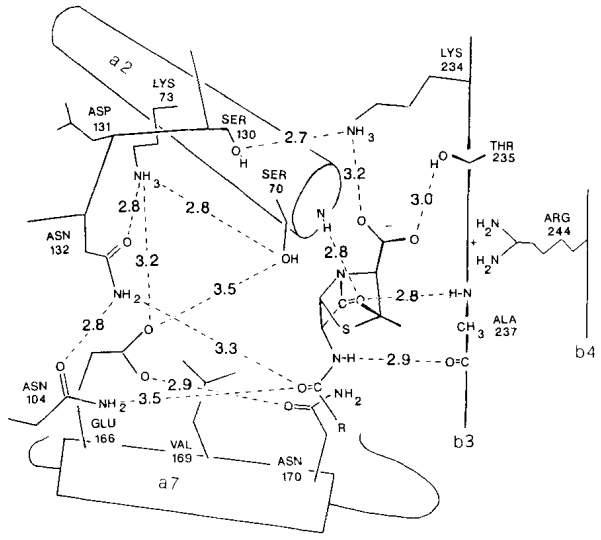

Fig. 7. Schematic diagram of distances (in Å) in penicillin binding site. The average of distances in both molecules is given.

turally homologous penicillin target DD-peptidase of *S.* R61.[16] In those 2.25 Å resolution maps, the serine-bound β-lactam moiety is clearly observed with the thiazolidine or dihydrothiazine ring at the top, and the acylamido substituent at the bottom, of a site having a geometry very similar to that seen here. A plausible model for positioning penicillin G in β-lactamase prior to acylation, and consistent with the crystallographic maps of the DD-peptidase complexes, is seen in Figure 8. The penicillin's carboxyl group at C3 (or C4 in cephalosporins) could initially be drawn to an exposed Arg-244 on the b3 β-strand. Here additional attractions for the carboxyl would be Lys-234, somewhat more exposed than Lys-73, and also the hydrogen-binding hydroxyl of the nearby Thr-235. The carbonyl bond of the β-lactam ring and the amide bond of the acylamido linkage are positioned to hydrogen bond in an antiparallel fashion to the backbone amide and carbonyl groups of residue 237, the side chain of which need not be, and is not, conserved. In this orientation the amide of 237 and the partial positive charge of the a2 helix dipole form part of a so-called oxyanion hole,[50] seen too in the mapping of complexes of the penicillin target DD-peptidase. The amide of Ser-70 can also attract the β-lactam carbonyl, and the amide thereby completes the formation of the oxyanion hole, as suggested by Herzberg and Moult.[7] With the β-lactam's carboxyl and ring carbonyl thus fixed, the β-lactam ring is aligned for α-face attack[51] by Ser-70. An alternative ion-pair interaction of the β-lactam's carboxylate solely with the Lys-73 in the conserved Ser-x-x-Lys peptide has been postulated in PBPs.[52,53] Our modeling shows this interaction is difficult to justify because the carboxyl would lie in the vicinity of the like-charged carboxyl of conserved Glu-166, a hydrogen bond to the 237 carbonyl would be lost, and the conserved functionalities at 234 and 235 would be left with no role in substrate binding.

An acylamido substituent would lie at the *bottom* of the binding site. Because Asn-170 projects upward from the a7 helix, the substituent must remain relatively exposed alongside the b3 β-strand. (A similar exposed position for acylamide substitutents was seen experimentally for β-lactam complexes with the *S.* R61 DD-peptidase.[16]) A result is the ability of β-lactamases in general to hydrolyze β-lactams with a variety of very large substituents beyond the acylamide. We can now begin to understand why the *S. aureus* β-lactamase,[7] with a unique insertion at 238/240 on the b3 strand of an isoleucine side chain, is less effective in hydrolyzing β-lactams with branched side chains at the α-carbon of the acylamide.[2,54–56]

It is unusual that the perimeter of this binding site contains no fewer than four tyrosines (105, 129, 241, and 274). Of these, Tyr-105 and 274 are closer than the others to the substrate, and they are possibly the sites of iodination in the enhanced iodine sensitivity of the enzyme during the binding of the poorer β-lactam substrates.[55]

Structural Considerations in Catalysis and Inhibition

In these surroundings at pH 5.5 the hydroxyl group of the reactive Ser-70 could be activated in at least two ways: First, the dipole moment of helix a2 provides a formal half positive charge[57] which may assist in lowering the p*K* of the hydroxyl proton. Such an effect is seen also in papain, where the reactive Cys-25 is at the N-terminus of a helix.[58] Second, the charged amino group of Lys-73, only 2.8 Å from Ser-70, may repel and orient the serine's proton for direct transfer to the β-lactam during formation of the acyl intermediate. A proton relay path via another residue is not obvious (see Fig. 7). β-Lactamase is unlike the classical serine enzymes in that no histidine is available for base-catalyzed activation of the serine hydroxyl. The conserved carboxyl groups of Asp-131 and Asp-233 are much too distant for interaction with Ser-70. The carboxyl of glutamic acid 166 is about 3.5 and 3.2 Å from Ser-70 and Lys-73, respectively. Glu-166 could play a direct role in base catalysis if brought closer to Ser-70 by conformational changes or vibrational modes. Perhaps the often-invoked "floppiness" of β-lactamases,[4]if occurring in the a7 helix/loop region, would facilitate this acylation. Glu-166 could also assist deacylation by hydrogen bonding to an approaching water molecule prior to nucleophilic attack as suggested for the *S. aureus* enzyme,[7] though

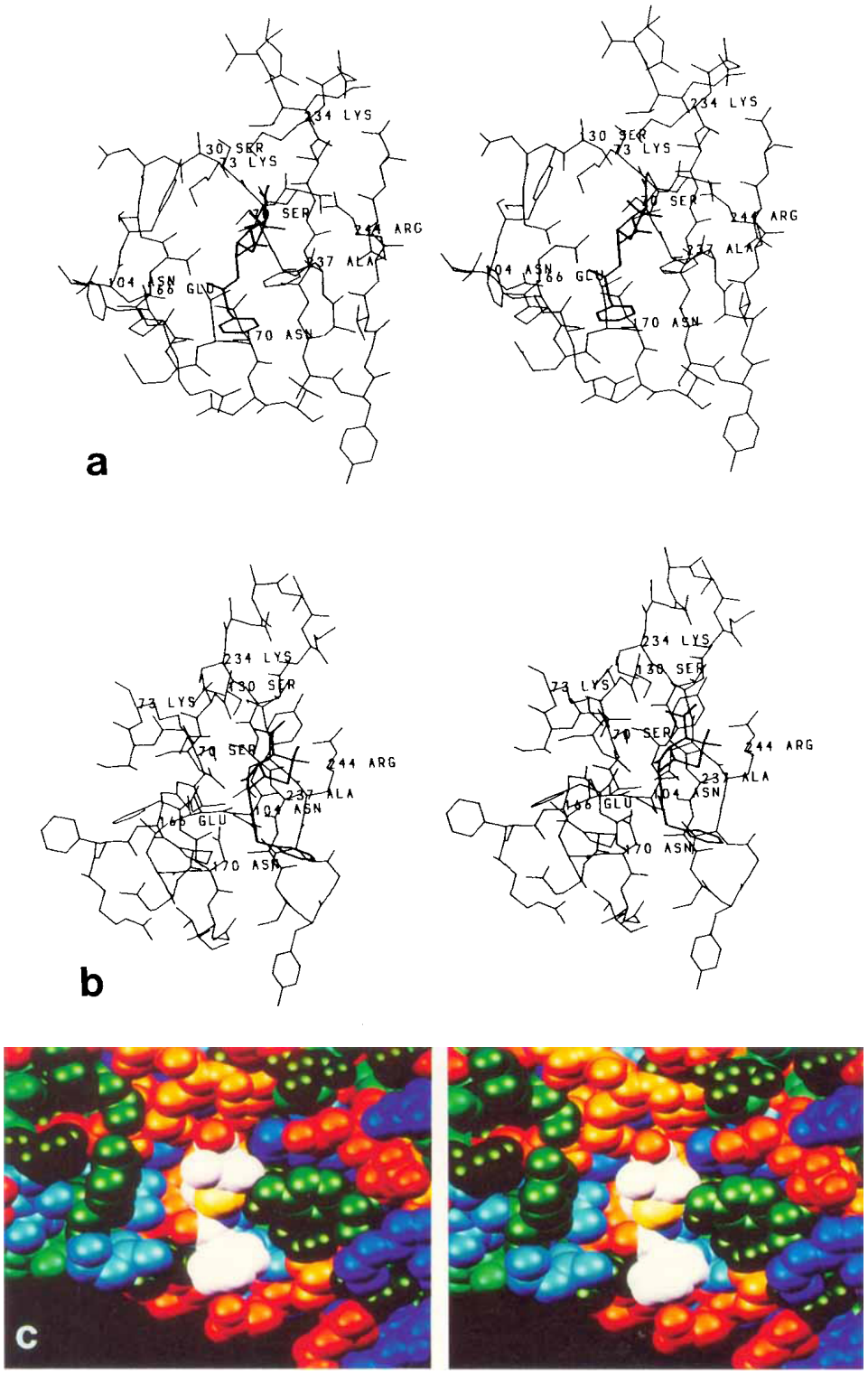

Fig. 8 **(a)** Atomic structure near β-lactam binding site. Penicillin G is positioned for α-face acylation by reactive Ser-70, with hydrogen bonding of β-lactam carbonyl to amides of Ser-70 and Thr-237. The carbonyl of Thr-237 hydrogen bonds to the acylamide NH group of the penicillin, whose C3 carboxyl group interacts with the side chains of conserved Lys-234, Thr-235, and Arg-244. Of the two known thiazolidine ring conformations, the 3a-COOH equatorial (Boyd)[51,52] or open (Christensen et al.)[70] conformation is used, in which the torsion angle defined by the β-lactam bond and the C3-C carboxyl bond is 125°. Considerable side chain flexibility has been observed in penicillin G.[71] The native enzyme conformation shown here was determined in substrate-free crystals at pH 5.5; side chain rotations may occur when substrate enters the binding site or when the pH is changed. Active site conformations of both molecules in the asymmetric unit are similar; atoms within 9 Å of the Ser-70 gamma-oxygen match with an RMS deviation of 0.22 Å. **(b)** View from left of binding site, showing α-face of β-lactam in relation to Ser-70 and Glu-166. **(c)** Space-filling VIEW diagram of enzyme groups near penicillin G, in the orientation of Figure 3. Penicillin color scheme: sulfur (yellow), oxygen (red), nitrogen (blue), remainder (white). Enzyme: red: Glu, Asp; orange: Ser, Thr; dark blue: Lys, Arg, His; light blue: Asn, Gln; yellow: Met; dark green: Leu, Ile, Val; green: Phe, Tyr, Trp; light green: Gly, Ala, Pro. Ala-237 and 238 are to the right of penicillin. (Courtesy of Mark Harris and David Chen, University of North Carolina.)

many groups (Asn-104, Asn-132, and Asn-170) are available for this role.

Polarization of the β-lactam carbonyl bond prior to nucleophilic attack by Ser-70 is accomplished by the aforementioned hydrogen binding to the backbone amides of Ser-70 and Thr-237, leading to α-face attack on the β-lactam. To a lesser extent, the conserved Ser-130 could conceivably polarize the β-lactam carbonyl bond, but it is difficult to position the β-lactam so that both Ser-70 and Ser-130 are correctly oriented with respect to the β-lactam carbonyl bond. Any hypothesis for the role of the centrally located Ser-130 must take account, however, of the fact that it is may not be present in this position in the Class C β-lactamases (see below).

If one accepts that only the attractions utilizing the C3(4) carboxyl and β-lactam carbonyl are sufficient for initial recognition, that is, that the acylamido amide hydrogen bond to the backbone carbonyl of residue 237 is *not* required, then the binding of β-lactams without C6(7) substituents, such as penicillanic acid sulfone or clavulanic acid, can be better understood. The variable side chain of residue 237 could contact large β-face substituents at C2(3) or the β oxygen of a sulfone. β-Halo substituents at C6(7) are more distant from 237, but may be in contact with larger enzymic side chains at 237. Especially interesting is that the nitrogen of the β-lactam ring is not explicitly used here, so that the reported binding of cyclobutanones to the DD-peptidase and β-lactamases[15,59] can be rationalized.

The proposal by Jones et al.[60] that the ring nitrogen of a penicilloate inhibitor is directly protonated by Lys-73 is inconsistent with the long 5.3 Å distance between the two groups. Recurring Arg-244 appears to be a new player in β-lactamase inactivation. In its location near the ring's carboxylate group, it is the most likely candidate as the base in the reaction of β-lactamases with sulfone or clavulanate-type inhibitors.[5,6] Clavulanates's reactive double bond at C2 would be about 3 Å from Arg-244, which is much closer than Lys-73 or Lys-234. The only known β-lactamase without arginine at position 244 (*S. albus* G with Asn) is less effectively inhibited by clavulanate. The number of turnovers before inactivation is 20,000 for the *S. albus* G enzyme compared to 200–400 for other β-lactamases.[61]

A brief comparison of this catalytic architecture with that in the penicillin-inhibited DD-peptidase was recently reported by Knox and Kelly,[62] who noted that the two active sites are geometrically very similar, that β-lactams can be bound in the same way to each site, but that the active site of the DD-peptidase is generally more hydrophobic in ways which could hinder hydrolysis of acyl intermediates.

β-Lactamase Variants and Mutants

In addition to the β-lactamase of *B. licheniformis* strain 749/C, another β-lactamase from strain 6346/C has also been well characterized.[54,56,63] The substrate profiles of the two enzymes are very different, as are their specific activities and Michaelis constants for representative substrates. The physiological efficiency, the ratio of V_{max} to K_m, is approximately the same for each enzyme, however. Substitution of the five 6346/C amino acids changes into this 749/C tertiary structure does little to explain the catalytic differences in the two β-lactamases, as the changes are quite distant from the binding site: Gln for Arg-191 in 749/C, Val for Met-287, Glu for Asn-293, Ser for Gly-294, and another change thought to be in the N-terminal region.[18]

More recently, site-directed mutagenesis was used by Fink et al.[64] to substitute the conserved Lys-234 with glutamic acid. That the mutant shows a 10-fold increase in K_m and a 200-fold decrease in V_{max} supports our belief that a positive group at position 234 of β-strand b3 is important for attracting and orienting the C3(or C4) carboxyl group of β-lactams, or the sulfate group of monobactams. In the β-lactamase I from *B. cereus* 569/H, Madgwick and Waley[47] have changed Lys-73 to Arg with significant, though not total, loss of activity. The more diffuse charge of the Arg may reduce its ability to orient or polarize the proton of Ser-70, and its multidentate nature may allow it to take on alternative hydrogen bondings. The change of Glu-166 to Gln, with loss of activity, was suggested to support the view that Glu-166 deprotonates Ser-70 in deacylation.

Many variants of the Class A β-lactamases encoded by the TEM-type plasmid in *E. coli* have been discovered.[65] Although the X-ray structure of the TEM β-lactamase is not known to useful resolution,[9] these TEM variants can also be analysed by examining the homologous *B. licheniformis* enzyme structure. An early single-site TEM mutant, found by Hall and Knowles[48] by selecting for cultures with increased resistance to cephalosporin C relative to penicillin G, is thought to contain threonine instead of alanine at position 237. We see that this residue is at a critical location in the binding site because its main chain atoms can hydrogen bond to the β-lactam, and the side chain of residue 237 would be close to the thiazolidine or dihydrothiazine rings of β-lactams.

By site-directed mutagenesis of the TEM β-lactamase Dalbadie-McFarland et al.[66] reversed the active site dipeptide Ser–Thr (present also in the *B. licheniformis* enzyme) to Thr–Ser with a resulting loss of activity, presumably because the serine is displaced by 4 Å to the topside of helix a2, where it would be too distant from a substrate anchored to the b3 strand. Schultz and Richards[67] report replacing Thr-71 with all possible amino acids. Only mutants with Tyr, Trp, Phe, Arg, Lys, or Asp at position 71 failed to display full activity on the three β-lactams tested (ampicillin, benzylpenicillin, 6-aminopenicillanic acid). From this tertiary structure it is

TABLE IX. Class C Changes in the Class A Structure

Position	Difference	Possible location in 3-D structure (Class A numbering)
114/115	Insertion, 26 residues	Left surface of enzyme between a3 and a4
130	Ala for conserved Ser	Binding site loop between a4 and a5
130/131	Insertion, 2 residues	Binding site loop
144/145	Insertion, 25 residues	Back surface between a5 and a6
160/161	Insertion, 5 residues	Back, between a6 and small β-strand
169/174	Deletion, 6 residues	Bottom of binding site
193/194	Insertion, 6 residues	Top rear at end of a8
233	His for conserved Asp	Top right side of binding site on b3 strand
228/229	Insertion, 28 residues	Top front surface between a10 and b3

clear that none of the substitutions at Thr-71 would sterically prevent substrate entry and binding. But because Thr-71 is buried in the enzyme between the a2 helix and the b3 strand, imposition of larger or charged side chains into the confined volume could cause a movement of helix a2 relative to the substrate-binding b3 strand. Alanine-69, on the other hand, is a better candidate for mutagenesis because it is on the substrate side of the serine-containing helix, rather than behind the helix as is Thr-71. Recently, Oliphant and Struhl[68] reported that a random selection procedure found several TEM mutants at position 69 which showed an increased resistance to the inhibitors clavulanate and sulbactam.

Comparison with Class C β-Lactamases

A three-dimensional structure of a Class C β-lactamase is not available, although crystallographic work is in progress.[10,69] On the basis of quantitative sequence alignment of Class C with Class A β-lactamases,[13] we can now attempt to relate Class C sequence differences to the known Class A tertiary structure. The larger Class C molecule contains six major insertions which are summarized in Table IX; their possible locations in the molecule can be described with the aid of Figure 3. For example, a 26-residue fragment inserted at 114/115 will be far from the β-lactam binding site on the left surface of the enzyme between the a3 and a4 helices. At 193/194 is a 6-residue peptide on the top surface of the molecule after helix a8. Five insertions, all probably surface runs between rigid secondary structure elements, would be unlikely to influence function. However, a sixth insert, a short Asn–Ser dipeptide between 130/131, because of its introduction into the binding site, and the noteworthy exchange at position 130 of the conserved Class A serine for an alanine, may both cause changes in catalytic behavior.

A factor which may alter substrate specificity is the deletion of six residues (equivalent to 169–174) in the bottom of the binding site where β-lactam side chains are expected to lie; a shortened a7 loop in the Class C enzymes would no longer contain the hydrophobic Leu-169 conserved in the Class A β-lactamases. Just prior to this deletion, the conserved Class A Glu-166 is replaced by a shorter aspartic acid side chain, which might be more distant from the acyl intermediate. These changes in the a7 helix/loop would tend to enlarge the space available to β-lactam substrates.

APPENDIX: THE RELATIONSHIP BETWEEN EULERIAN ANGLES AND A ROTATION AND AXIS

P.C. Moews and D.J. Moews

In order to derive the relationships between the molecules in the asymmetric unit, expressions relating a rotation axis and an angle and an orthogonal rotation matrix were developed and are given in Table X. These expressions are applicable both to the molecules related by the space group operations and to the molecules related by noncrystallographic symmetry. The conversion between Eulerian angles and rotation matrices which defines the conventions used in this paper are also given in Table X.

The values of the Eulerian angles which relate the different molecules in the unit cell depend upon the choice of orthogonalization matrix. The orthogonalization matrix chosen for this study was

$$\begin{bmatrix} 1 & 0 & \cos\beta \\ 0 & 1 & 0 \\ 0 & 0 & \sin\beta \end{bmatrix}$$

The expressions in Table X can now be used to derive the Eulerian angles relating the various molecules in the unit cell (see Table XI). For example, the molecule related by noncrystallographic symmetry is rotated 180° about a^* and after orthogonalization a^* becomes [sin(β) 0.0 -cos(β)]. We have a rotation (180°) and an axis (0.9681 0 0.2504); and the corresponding Eulerian angles are $\alpha = 0°$, $\beta = 151°$, $\gamma = 180°$. These values were confirmed by rotation function studies and by the determination of rotation matrices with a three-dimensional display terminal.

Table X. Relationship Between Various Forms of Rotational Parameters

Rotation by χ around axis $(l_1,l_2,l_3) = \vec{l}$, $(|\vec{l}| = 1)$, to rotation matrix $[m_{ij}]$

$$m_{ij} = \begin{bmatrix} \cos\chi + l_1^2(1-\cos\chi), & l_1l_2(1-\cos\chi) - l_3\sin\chi, & l_1l_3(1-\cos\chi) + l_2\sin\chi \\ l_1l_2(1-\cos\chi) + l_3\sin\chi, & \cos\chi + l_2^2(1-\cos\chi), & l_2l_3(1-\cos\chi) - l_1\sin\chi \\ l_1l_3(1-\cos\chi) - l_2\sin\chi, & l_2l_3(1-\cos\chi) + l_1\sin\chi, & \cos\chi + l_3^2(1-\cos\chi) \end{bmatrix}$$

Rotation matrix $[m_{ij}]$ to rotation by χ around axis $(l_1,l_2,l_3) = \vec{l}$, $|\vec{l}| = 1$

$$\chi = \cos^{-1}\left\{\frac{m_{11} + m_{22} + m_{33} - 1}{2}\right\}$$

$$l_1 = \frac{m_{32} - m_{23}}{2\sin\chi}, \quad l_2 = \frac{m_{13} - m_{31}}{2\sin\chi}, \quad l_3 = \frac{m_{21} - m_{12}}{2\sin\chi}$$

Rotation matrix $[m_{ij}]$ to Euler angles (α, β, γ)

$$\beta = \cos^{-1} m_{33}$$

$$(\beta = 0, \pi) \quad \begin{bmatrix} \gamma = 0 \\ \alpha \text{ from } \cos\alpha = \dfrac{m_{11}}{m_{33}}, \ \sin\alpha = \dfrac{m_{21}}{m_{33}} \end{bmatrix}$$

$$(\beta \neq 0, \pi) \quad \begin{bmatrix} \gamma \text{ from } \cos\gamma = -\dfrac{m_{31}}{\sin\beta}, \ \sin\gamma = \dfrac{m_{32}}{\sin\beta} \\ \alpha \text{ from } \cos\alpha = \dfrac{m_{13}}{\sin\beta}, \ \sin\alpha = \dfrac{m_{23}}{\sin\beta} \end{bmatrix}$$

Euler angles (α, β, γ) to orthogonal rotation matrix $[m_{ij}]$

$$m_{ij} = \begin{bmatrix} \cos\gamma\cos\beta\cos\alpha - \sin\gamma\sin\alpha, & -\sin\gamma\cos\beta\cos\alpha - \cos\gamma\cos\alpha, & \sin\beta\cos\alpha \\ \cos\gamma\cos\beta\sin\beta + \sin\gamma\cos\alpha, & -\sin\gamma\cos\beta\sin\alpha + \cos\gamma\cos\alpha, & \sin\beta\sin\alpha \\ -\cos\gamma\sin\beta, & \sin\gamma\sin\beta, & \cos\beta \end{bmatrix}$$

TABLE XI. Eulerian Angles Which Relate the Molecules in the A- and B-Form Cells of the β-Lactamase Crystals

Molecule*	α	β	γ
1(base)	0°	0°	0°
2	0°	180°	0°
3	0°	151°	180°
4	180°	29°	0°

*Molecules 1 and 3 form the asymmetric unit; molecules 2 and 4 are generated by the symmetry elements of the space group.

The angle and axis formulation is a useful one because if two orientations are nearly the same, this is always apparent from the axis and angle relationship, even though two similar orientations can have quite different Eulerian angles. If the relation between two different orientations is expressed as a rotation and an axis the minimum rotation required to superimpose the two orientations can be calculated (see Table III). A program which relates a number of conventions for the expression of rotational relationships, as well as those listed in Table X, is available from the authors.

ACKNOWLEDGMENTS

This work was supported by Grant GM-37742 to JRK from the National Institutes of Health, and, in part, by the American Cyanamid, Becton-Dickinson, Burroughs-Wellcome, Hoffmann-LaRoche, Lilly, Merck, Procter & Gamble, and Upjohn companies. The work in Liège was supported by the Fonds de la Scientific Medicale (contracts 3.4507-83 and 3.4522-86), the Belgian Government (Action Concertee contract 86/91-90), the Fonds de la Recherche de la Faculte de Medecine, Universite de Liège, and the CEE (contract BAP-0197-B). For assistance with X-ray data collection we thank Jean-Pierre Wery, Haiching Zhao, and the staff of the University of Virginia Multiwire Area X-Ray Diffractometer Facility. Computations were performed at the University of Connecticut Computer Center, the Pittsburgh Supercomputing Center through Grant NIH U41RR04154, and at the National Supercomputer Facility at the Center for Theory and Simulation at Cornell University. Figures 3a and 8c were generously supplied by Mark Harris and David Chen of the Department of Computer Sciences at the University of North Carolina. For helpful discussions we wish to thank A.T. Brünger, C.W. David, J.A. Kelly, D.J. Moews, R.F. Pratt, and J.K. Mohana Rao.

REFERENCES

1. Kelly, J.A., Dideberg, O., Charlier, P., Wery, J.P., Libert, M., Moews, P.C., Knox, J.R., Duez, C., Fraipont, C., Joris, B., Dusart, J., Frère, J.-M., Ghuysen, J.M. On the origin of bacterial resistance to penicillin: Comparison of a β-lactamase and a penicillin target. Science 231:1429–1431, 1986.
2. Coulson, A. β-Lactamases: Molecular studies. Biotechnol. Gen. Eng. Rev. 3:219–253, 1985.
3. Frère, J.-M., Joris, B. Penicillin-sensitive enzymes in peptidoglycan biosynthesis. CRC Crit. Rev. Microbiol. 11: 299–396, 1985.
4. Fink, A.L. The molecular basis of β-lactamase catalysis and inhibition. Pharma. Res. 55–96, 1985.
5. Knowles, J. R. Penicillin resistance: The chemistry of β-lactamase inhibition. Accts. Chem. Res. 18:97–102, 1985.
6. Pratt, R.F. β-Lactamase inhibitors. In: "Design of Enzyme Inhibitors as Drugs" (Sandler, M., Smith, H.J., eds.). Oxford University Press. 1988:178–205.
7. Herzberg, O., Moult, J. Bacterial resistance to β-lactam antibiotics: Crystal structure of β-lactamase from *Staphylococcus aureus* PC1 at 2.5 Å resolution. Science 236:694–701, 1987.
8. Dideberg, O., Charlier, P., Wèry, J.-P., Dehottay, P., Dusart, J., Erpicum, T., Frère, J.-M., Ghuysen, J.-M. The crystal structure of the β-lactamase of *Streptomyces albus* G at 0.3 nm resolution. Biochem J. 245:911–913, 1987.
9. Knox, J.R., Kelly, J.A., Moews, P.C., Murthy, N.S. 5.5Å crystallographic structure of penicillin β-lactamase and radius of gyration in solution. J. Mol. Biol. 104:865–875, 1976.
10. Charlier, P., Dideberg, O., Frère, J.-M., Moews, P.C., Knox, J.R. Crystallographic data for the β-lactamase from *Enterobacter cloacae* P99. J. Mol. Biol. 171:237–238, 1983.
11. Samraoui, B., Sutton, B.J., Todd, R.J., Artymiuk, P.J., Waley, S.G., Phillips, D.C. Tertiary structural similarity between a class A β-lactamase and a penicillin-sensitive D-alanyl carboxypeptidase-transpeptidase. Nature (London) 320:378–380, 1986.
12. Sutton, B.J., Artymiuk, P.J., Cordero-Borboa, A.E., Little, C., Phillips, D.C., Waley, S.G. An X-ray-crystallographic study of β-lactamase II from *Bacillus cereus* at 0.35 nm resolution. Biochem. J. 248:181–188, 1987.
13. Joris, B., Ghuysen, J.M., Dive, G., Renard, A. Dideberg, O., Charlier, P., Frère, J.-M., Kelly, J.A., Boyington, J.C., Moews, P.C., Knox, J.R. The active-site-serine penicillin-recognizing enzymes as members of the *Streptomyces* R61 DD-peptidase family. Biochem. J. 250:313–324, 1988.
14. Wang, B.C. Resolution of phase ambiguity in macromolecular crystallography. Methods Enzymol. 115:90–111, 1985.
15. Kelly, J.A., Knox, J.R., Moews, P.C., Hite, G.J., Bartolone, J.B., Zhao, H., Joris, B., Frère, J.-M., Ghuysen, J.-M. 2.8 Å Structure of penicillin-sensitive D-alanyl carboxypeptidase-transpeptidase from *Streptomyces* R61 and complexes with β-lactams. J. Biol. Chem. 260:6449–6458, 1985.
16. Kelly, J.A., Knox, J.R., Zhao, H., Frère, J.-M., Ghuysen, J.M. Crystallographic mapping of β-lactams bound to a DD-peptidase. J. Mol. Biol. 209:281–295, 1989.
17. Neugebauer, K., Sprengel, R., Schaller, H. Penicillinase from *Bacillus licheniformis:* Nucleotide sequence of the gene and implications for the biosynthesis of a secretory protein in a Gram-positive bacterium. Nucl. Acids Res. 9:2577–2588, 1981.
18. Thatcher, D.R. β-Lactamase (*Bacillus licheniformis*). Methods Enzymol. 43:640–698, 1975.
19. Dideberg, O., Libert, M., Frère, J.-M., Charlier, P., Zhao, H.C., Knox, J.R. Crystallization and preliminary x-ray data for the exocellular β-lactamase of *Bacillus licheniformis* 749/C. J. Mol. Biol. 181:145–146, 1985.
20. North, A.C.T., Phillips, D.C., Mathews, F.S. A semi-empirical method of absorption correction. Acta Crystallogr. A24:351–359, 1968.
21. Blow, D.M., Crick F.H.C. The treatment of errors in the isomorphous replacement method. Acta Crystallogr. 12: 794–802, 1959.
22. Williams, T.V. A man-machine interface for interpreting electron density maps. Ph.D. Dissertation,, University of North Carolina, 1982.
23. Sobottka, S.E., Cornick, G.G., Kretsinger, R.H., Rains, R.G., Stephens, W.A., Weissman, L.J. A MWPC x-ray diffractometer facility for protein crystallography. Nucl. Inst. Methods 220:575–581, 1984.
24. Crowther, R.A. The fast rotation function, In: "The Molecular Replacement Method" (Rossmann, M.G., ed.), Int. Sci. Rev. Ser., No. 13, New York: Gordon & Breach, 1972:173–178.
25. Fujinaga, M., Read, R.J. Experiences with a new transla-

tion-function program. J. Appl. Crystallogr. 20:517–521, 1987.
26. Stewart, J.M., Kruger, G.J., Ammon, H.L., Dickinson, C. Hall, S.R. The x-ray system of crystallographic programs. Technical Report TR-192, University of Maryland, 1972.
27. Adams, M.J., Haas, D.J., Jeffery, B.A., McPherson, A., Mermall, H.L., Rossmann, J., Schevitz, R.W., Wonacott, A.J. Low resolution study of L-lactate dehydrogenase. J. Mol. Biol. 41:159–188, 1981.
28. Jones, T.A. FRODO: a graphics fitting program for macromolecules. In: "Computational Crystallography" (D. Sayre, ed.). Oxford: Clarendon Press, 1982:303–317.
29. Konnert, J.H., Hendrickson, W. A Restrained-parameter thermal-factor refinement procedure. Acta Crystallogr. A36:344–350, 1980.
30. Brünger, A.T. A memory-efficient fast Fourier transformation algorithm for crystallographic refinement on supercomputers. Acta Crystallogr. A45:42–50, 1989.
31. Brünger, A.T., Karplus, M., Petsko, G.A. Crystallographic refinement by simulated annealing: Application to crambin. Acta Crystallogr. A45:50–61, 1989.
32. Brünger, A.T. X-PLOR (Version 1.5) Manual. The Howard Hughes Medical Institute and Department of Molecular Biophysics and Biochemistry, Yale University, 1988.
33. Read, R.J. Improved Fourier coefficients for maps using phases from partial structures with errors. Acta Crystallogr. A42:140–149, 1986.
34. Bhat, T.N. Calculation of an OMIT map. J. Appl. Crystallogr. 21:279–281, 1988.
35. Baker, E.N. Structure of azurin from *Alcaligenes denitrificans*. Refinement at 1.8Å resolution and comparison of the two crystallographically independent molecules. J. Mol. Biol. 203:1071–1095, 1988.
36. Kelly, J.A., Boyington, J.C., Moews, P.C., Knox, J.R., Dideberg, O., Charlier, P.C., Libert, M., Wery, J.P., Duez, C., Joris, B., Dusart, J., Frère, J.-M., Ghuysen, J.M. Crystallographic comparisons of penicillin-binding enzymes and studies of antibiotic binding. In: "Frontiers of Antibiotic Research, Takeda Science Foundation" (Umesawa, H., ed.), New York: Academic Press, 1987:327–337.
37. Knox, J.R., Kelly, J.A., Moews, P.C., Zhao, H., Moring, J., Rao, J.K.M., Boyington, J., Dideberg, O., Charlier, P., Libert, M. Crystallography of penicillin-binding enzymes. In: "Three-dimensional Structure and Drug Action" (Iitaka, I., Itai, A. eds.), Tokyo: University of Tokyo Press, 1987: 64–82.
38. Chou, P.Y., Fasman, G.D. β-Turns in proteins. J. Mol. Biol. 115:135–175, 1977.
39. Garnier, J., Osguthorpe, D.J. Robson, R. Analysis of the accuracy and implications of simple methods for predicting the secondary structure of globular proteins. J. Mol. Biol. 120:97–120, 1978.
40. Moews, P.C., Knox, J.R. Predicted secondary structures of four penicillin β-lactamases and a comparison with two lysozymes. Int. J. Pept. Protein Res. 13:385–393, 1979.
41. Pain, R.H., Virdin, R. The structural and conformational basis of β-lactamase activity. In: "β-Lactamases" (Hamilton-Miller, J.M.T., Simth, J.T., eds.). London: Academic Press, 1979:141–181.
42. Bunster, M., Cid, H. A model for the secondary structure of β-lactamases. FEBS Lett. 175:267–274, 1984.
43. Ambler, R.P. The structure of β-lactamases. Phil. Trans. Ry. Soc. London, Ser. B 289:321–331, 1980.
44. Coulson, A. Fourth β-Lactamase Workshop, Holy Island, UK (R. Virden, R. Pain, organizers), 1988.
45. Murthy, N.S., Braswell, E.H., Knox, J.R. The association behavior of β-lactamases in polyethylene glycol solutions. Biopolymers 27:865–881, 1987.
46. Richardson, J.S. The anatomy and taxonomy of protein folding. Adv. Prot. Chem. 34:167–339, 1981.
47. Madgwick, P.J., Waley, S.G. β-Lactamase I from *Bacillus cereus:* Structure and site-directed mutagenesis. Biochem. J. 248:657–662, 1987.
48. Hall, A., Knowles, J.R. Directed selective pressure on a β-lactamase to analyze molecular changes involved in development of enzyme function. Nature (London) 264:803–804, 1976.
49. Little, G., Emanuael, E.L., Gangnon, J., Waley, S.G. Carboxy groups as esential residues in β-lactamases. Biochem. J. 240:215–219, 1986.
50. Kraut, J. Serine proteases: Structure and mechanism of catalysis. Annu. Rev. Biochem. 46:331–359, 1977.
51. Boyd, D.B. Theoretical and physiochemical studies on β-lactam antibiotics. In: "Chemistry and Biology of β-Lactam Antibiotics" (Morin, R.B. Gorman, M., eds.), New York: Academic Press, Vol. 1, 1982:437–545.
52. Boyd, D.B. Computer-assisted molecular design studies of β-lactam antibiotics. In: "Frontiers of Antibiotic Research." New York: Academic Press, 1987:339–356.
53. Varetto, L., Frère, J.-M., Ghuysen, J.M. The importance of the negative charge of β-lactam compounds for the inactivation of the active-site serine DD-peptidase of *Streptomyces* R61. FEBS Lett. 225:218–222, 1987.
54. Pollock, M.R. Range and significance of variations among bacterial penicillinases. Ann. N.Y. Acad. Sci. 151: 502–515, 1968.
55. Citri, N., Pollock, M.R. The biochemistry and function of β-lactamase (penicillinase). Adv. Enzymol. 28:237–324, 1966.
56. Naylor, J.H.C. Structure-activity relationships in semisynthetic penicillins. Proc. R. Soc. London Ser. B 179:357–367, 1971.
57. Hol, W.G.J. The role of the α-helix dipole in protein function and structure. Prog. Biophys. Mol. Biol. 45:149–195, 1985.
58. Drenth, J., Kalk, K.H., Swen, H.M. Binding of chloromethyl ketone substrate analogues to crystalline papain. Biochemistry 15:3731–3738, 1976.
59. Lowe, G., Swain, S. Do β-lactam antibiotics require a β-lactam ring? In: "Recent Advances in the Chemistry of β-Lactam Antibiotics," London: Royal Society of Chemistry, 1985:209–221.
60. Jones, M., Buckwell, S.C., Page, M.I., Wigglesworth, R. A reversible inhibitor of β-lactamase I from *Bacillus cereus*. J. Chem. Soc. Chem. Commun. 1989:70–71.
61. Frère, J.-M., Dormans, C., Lenzini, V.M., Duyckaerts, C. Interaction of clavulanate with the β-lactamases of *Streptomyces albus* G and *Actinomadura* R39. Biochem. J. 207: 429–436, 1982.
62. Knox, J.R., Kelly, J.A. Crystallographic comparison of penicillin-recognizing enzymes. In: "Molecular Recognition: Chemical and Biochemical Problems" (Roberts, S. ed.), Royal Soc. Chem. 1989:46–55.
63. Pollock, M.R. Purification and properties of penicillinases from two strains of *Bacillus licheniformis:* A chemical, physiochemical and physiological comparison. Biochem. J. 94:666–675, 1965.
64. Fink, A.L., Ellerby, L.M., Escobar, W.A., Mitchinson, C. Wells, J.A. Site-directed mutagenesis studies on the role of lysine-234 in β-lactamase catalysis. Submitted.
65. Philippon, A., Labia, R., Jacoby, G. Extended-spectrum β-lactamases. Antimicrob. Ag. Chemother. 33:1131–1136, 1989.
66. Dalbadie-McFarland, G., Cohen, L.W., Riggs, A.D., Morin, C., Itakura, K., Richards, J.H. Oligonucleotide-directed mutagenesis as a general and powerful method for studies of protein function. Proc. Natl. Acad. Sci. U.S.A. 79:6409–6413, 1982.
67. Schultz, S.C., Richards, J.H. Site-saturation studies of β-lactamase: Production and characterization of mutant β-lactamases with all possible amino acid substitutions at residue 71. Proc. Natl. Acad. Sci. U.S.A. 83:1588–1592, 1986.
68. Oliphant, A., Struhl, L. Creating novel β-lactamases by random selection. Proc. Natl. Acad. Sci. U.S.A. In press.
69. Oefner, C. Fourth β-Lactamase Workshop, Holy Island, UK (R. Virden, R. Pain, organizers), 1988.
70. Christenson, J.G., Pruess, D.L., Talbot, M., Keith, D.D. Antibacterial properties of (2,3)-α- and (2,3)-β-methylene analogs of penicillin G. Antimicrob. Ag. Chemother. 32: 1005–1011, 1988.
71. Dexter, D.D., van der Veen, J.M. Conformations of penicillin G. J. Chem. Soc. Perkin I. 1978:185–190.